Treatment with eldecalcitol positively affects mineralization, microdamage, and collagen crosslinks in primate bone

Mitsuru Saito[a], Marc D. Grynpas[b], David B. Burr[c], Matthew R. Allen[c], Susan Y. Smith[d], Nancy Doyle[d], Norio Amizuka[e], Tomoka Hasegawa[e], Yoshikuni Kida[a], Keishi Marumo[a], and Hitoshi Saito[f]

[a]*Jikei University School of Medicine, Orthopedic Surgery Department, 3-25-8 Nishishinbashi, Minato-ku, Tokyo 105-8461, Japan*

[b]*Samuel Lunenfeld Research Institute, Mount Sinai Hospital, Toronto, Canada*

[c]*Department of Anatomy and Cell Biology, Department of Orthopaedic Surgery, Indiana University School of Medicine, Indianapolis, USA*

[d]*Bone Research, Charles River Laboratories Preclinical Services Montreal, Senneville, Quebec, Canada*

[e]*Division of Oral Health Science, Graduate School of Dental Medicine, Hokkaido University, Sapporo, Japan.*

[f]*Medical Science Department, Chugai Pharmaceutical Co., Ltd., Tokyo, Japan*

Running title: Eldecalcitol improves bone quality in primates

Total number of words: 4808

Total number of figures: 4

Corresponding Author:

Mitsuru Saito, MD, PhD.

Jikei University School of Medicine, Orthopedic Surgery Department, 3-25-8 Nishishinbashi, Minato-ku, Tokyo 105-8461, Japan.

Phone: +81-03-3433-1111 (ext. 3441); Fax: +8103-3459-9114; E-mail: xlink67@gol.com

Conflict of Interest:

MS has received research grants and/or consulting or speaking fees from Pfizer Inc., Eli Lilly Co., Ltd, Chugai Pharmaceutical Co., Ltd, Dai-ichi Sankyo Co., Ltd, and Asahi-Kasei Pharma Co., Ltd.

SYS and ND are fulltime employees of Charles River Laboratories.

HS is a fulltime employee of Chugai Pharmaceutical Co., Ltd.

Other authors have no conflict of interest.

Abstract

Eldecalcitol (ELD), an active form of vitamin D analog approved for the treatment of osteoporosis in Japan, increases lumbar spine bone mineral density (BMD), suppresses bone turnover markers, and reduces fracture risk in patients with osteoporosis. We have previously reported that treatment with ELD for 6 months improved the mechanical properties of the lumbar spine in ovariectomized (OVX) cynomolgus monkeys. ELD treatment increased lumbar BMD, suppressed bone turnover markers, and reduced histomorphometric parameters of both bone formation and resorption in vertebral trabecular bone. In this study, we elucidated the effects of ELD on bone quality (namely, mineralization, microarchitecture, microdamage, and bone collagen crosslinks) in OVX cynomolgus monkeys in comparison with OVX-vehicle control monkeys. Density fractionation of bone powder prepared from lumbar vertebrae revealed that ELD treatment shifted the distribution profile of bone mineralization to a higher density, and backscattered electron microscopic imaging showed improved trabecular bone connectivity in the ELD-treated groups. Higher doses of ELD more significantly reduced the amount of microdamage compared to OVX-vehicle controls. The fractionated bone powder samples were divided according to their density, and analyzed for collagen crosslinks. Enzymatic crosslinks were higher in both the high-density (≥2.0 mg/mL) and low-density (<2.0 mg/mL) fractions from the ELD-treated groups than in the corresponding fractions in the OVX-vehicle control groups. On the other hand, non-enzymatic crosslinks were lower in both the high- and low-density fractions. These observations indicated that ELD treatment stimulated the enzymatic reaction of collagen crosslinks and bone mineralization, but prevented non-enzymatic reaction of collagen crosslinks and accumulation of bone microdamage. Bone anti-resorptive agents such as bisphosphonates slow down bone remodeling so that bone mineralization, bone microdamage, and non-enzymatic collagen crosslinks all increase. Bone anabolic agents such as parathyroid hormone decrease bone mineralization and bone microdamage by stimulating bone remodeling. ELD did not fit into either category. Histological analysis indicated that the ELD treatment strongly suppressed bone resorption by reducing the number of osteoclasts, while also stimulating focal bone formation without prior

bone resorption (bone minimodeling). These bidirectional activities of ELD may account for its unique effects on bone quality.

Keywords: vitamin D, bone quality, bone mineralization, bone microdamage, bone microarchitecture, collagen crosslinks

1. Introduction

Bone mineral density (BMD) and bone quality are two major components of bone strength. Bone quality consists of bone geometry, bone microarchitecture, bone microdamage, bone mineralization, and bone material properties. These determinants of bone quality are regulated by bone turnover and the degree of oxidative stress [1][2][3]. Eldecalcitol [1α,25-dihydroxy-2β-(3-hydroxypropyloxy)vitamin D_3; ELD], an analog of calcitriol [1α,25-dihydroxyvitamin D_3; $1,25(OH)_2D_3$], has been demonstrated to increase bone mass, to suppress bone turnover markers, and to enhance bone strength in rodents [4][5] and in non-human primates [6]. ELD suppresses RANKL expression in osteoblasts [7], suppresses differentiation of preosteoclasts to mature osteoclasts [8], stimulates cell-migration of osteoclast precursor monocytes [9], and therefore, reduces the number of mature osteoclasts on the bone surface. A 3-year randomized, double-blind, active-comparator, clinical trial of ELD in postmenopausal women with osteoporosis demonstrated that ELD significantly decreased the incidence of vertebral fractures and wrist fractures, increased both lumbar spine and hip BMD, and suppressed bone turnover markers in comparison to alfacalcidol (1α-hydroxyvitamin D_3) [10]. Deterioration of bone architecture in the hip was reduced by ELD treatment [11]. A post-hoc analysis revealed that, compared with placebo, ELD reduced incidence of vertebral fractures by approximately 50% in osteoporotic patients with prevalent fractures [12]. This series of results raises an important question. Treatment with ELD increases lumbar spine BMD by only 3% per year and reduces bone turnover markers by approximately 30% per year compared with the pretreatment level. On the other hand, treatment with most bisphosphonates increases lumbar spine BMD by more than 5% per year and reduces bone turnover markers by 50%–60% per year. Despite its more restrained effects on BMD and bone turnover markers, the anti-fracture activity of ELD is comparable to that of bisphosphonates [13]. These differences suggest that in addition to the effects of ELD on BMD and bone turnover markers, the anti-fracture activity of ELD treatment may be attributable to improved bone quality.

We have previously shown that treatment with 0.1 μg/kg/day and 0.3 μg/kg/day of ELD increases lumbar spine and hip BMD, suppresses bone turnover markers, and eventually increases bone mechanical properties of

lumbar vertebrae in ovariectomized (OVX) cynomolgus monkeys [6]. Unlike rodent models, ovariectomized non-human primates have a skeletal anatomy and bone material properties in terms of collagen crosslink formation similar to those of postmenopausal women, with intracortical bone remodeling and increased bone turnover and bone loss associated with estrogen deficiency [14][15].

Regarding bone material properties, collagen crosslinking is an independent determinant of bone strength [3][16]. Bone collagen crosslinks can be divided into immature and mature enzymatic crosslinks and glycation- or oxidation-induced non-enzymatic senescent crosslinks (advanced glycation end products, AGEs). Enzymatic crosslink formation has positive effects on the mechanical properties of bone, conferring flexibility without brittleness [17][18][19][20][21]. In contrast, AGE crosslinks result in brittle collagen fibers, thereby leading to microdamage and bone fragility [17][22][23]. AGE crosslinks are formed by oxidation or glycation reactions in a time-dependent manner, and are regulated by tissue turnover rate [22][24], the degree of oxidative stress [25][26], or glycation level [17][23]. Pentosidine is a well-established intermolecular crosslinking AGE and is used as a surrogate marker of total AGE formation [17][26][27][28][29][30].

In this study, in order to evaluate the effect of ELD on bone material and structural properties, we analyzed bone mineralization, bone microarchitecture, bone microdamage, immature and mature enzymatic collagen crosslinks, and AGEs in the bone samples collected for the OVX cynomolgus monkey study previously reported [6].

2. Materials and Methods

2.1 Animals and experimental design

All animal procedures were as previously reported [6]. Briefly, 40 female cynomolgus monkeys, at least 9 years of age, were housed in pairs and fed twice daily with food supplements and/or fresh fruit, and had free access to water. The animal room environment was controlled, with settings targeted at a temperature of 22±3°C, humidity of 50±20%, photoperiod of 12 h light and 12 h dark, and 12 air changes per hour. Two separate experiments were conducted, one experiment using a dose of 0.1 μg/kg ELD and a corresponding OVX-vehicle control group and the other experiment using 0.3 μg/kg ELD and a corresponding OVX-vehicle

control group. Medium chain triglyceride was used for the vehicle solution. For each experiment, 20 animals were randomly assigned to either the OVX-vehicle control group or the ELD group (n = 10/group). The groups were balanced to ensure that age, body weights, whole body bone mineral content (BMC), and lumbar spine BMD were equivalent across groups within each experiment.

Daily treatment started the day following ovariectomy, with either vehicle alone (OVX-Veh1 or OVX-Veh2) or ELD (at 0.1 µg/kg in the first experiment or 0.3 µg/kg in the second experiment), and continued for 6 months. Animals were euthanized under anesthesia by exsanguination, and bone samples were excised. The study was approved by the Charles River Montreal Animal Care Committee and was performed in a facility accredited by the Association for Assessment and Accreditation of Laboratory Animal Care.

2.2 Density fractionation

Density fractionation was carried out as previously reported [31][32][33]. Briefly, the third lumbar vertebrae (L3) were crushed and washed in 0.2M Tris-HCl buffer (pH7.4) to remove bone marrow, lyophilized, and then defatted in 2:1 (v:v) chloroform:methanol solution. The bone pieces were then pulverized in a percussion mill cooled in liquid nitrogen (Spex Freezer Mill; Spex Sampleprep, Metuchen, NJ, USA) and then sieved in a sonic sifter to separate bone particles less than 20 µm in size. The bone powder was then chemically "fractionated" (into seven fractions from < 1.8 g/mL to > 2.1 g/mL) in a bromoform–toluene mixtures by a method of stepwise centrifugation [33]. Approximately 200 mg of the sieved bone was added to a polyallomer centrifuge tube containing 35 mL of a 1.95 g/mL density solution (calibrated with sink floats) for cancellous bone. The tubes were sonicated to achieve a homogeneous suspension of the powder, which was then centrifuged at 10,000 rpm for 30 min in a Beckman L5-55 ultracentrifuge using an SW20 rotor. The density of the supernatant was adjusted to 1.9 g/mL via the addition of toluene, and the modified solution was re-centrifuged. In a similar way, each precipitate obtained from a solution of progressively decreasing density (in 0.05 g/mL steps) was collected. For the range of mineral densities greater than 1.95 g/mL, the precipitates obtained from an initial 2.0 g/mL density solution was re-suspended in a solution of density 2.1 g/mL. Similarly, successive centrifugation of the precipitate at progressively higher densities (0.05 g/mL steps) determined the higher density fractions.

Removal of organic solvent from the series of density fractions was achieved by a "rinse" centrifugation in 100% ethyl alcohol. The samples were then dried in a desiccator at room temperature. The contribution of each fraction, relative to the original weight of unfractionated bone, was calculated to determine a mineralization profile for each group.

2.3 Bone microdamage assessment

The fourth lumbar vertebrae (L4) were processed for microdamage assessment by bulk staining in basic fuchsin. Using 1% basic fuchsin dissolved in increasing concentrations of ethanol, specimens were stained according to the following schedule: 4 h in 80%, 4 h in 80%, 4 h in 95%, overnight in 95%, 4 h in 100%, and 4 h in 100%. At each step, the solution was replaced with fresh solution after 2 h. Bones were placed under vacuum (20 in Hg) for all stages during the day and left on the bench top overnight. Following staining, bones were washed twice in 100% ethanol (5 min each), and placed in 100% methylmethacrylate (MMA; Sigma-Aldrich) under vacuum for 4 h. Specimens were then transferred to a solution of MMA + 3% dibutyl phthalate (DBP; Sigma-Aldrich) for 3–7 days under vacuum and then embedded using MMA + DBP + 0.25% catalyst (Perkadox 163; Akzo Nobel Chemicals, Pasadena, USA). Mid-sagittal sections 80–100 μm thick were cut using a diamond wire saw (Histosaw; Delaware Diamond Knives, Inc., DE, USA).

Histological measurements were made using a microscope interfaced with Bioquant analysis software (Bioquant OSTEO 7.20.10; Bioquant Image Analysis Co., TN, USA). Measurements were carried out on two sections per animal to increase the probability of finding cracks. A region of interest approximately 5 × 5 mm, located 1 mm below the cranial plateau, was used for sampling, and linear microcracks were identified as previously described [34]. Measurements included crack length (Cr.Le; 200× magnification) (μm) and crack number (Cr.N; 100× magnification), with calculations of crack density (Cr.Dn = Cr.N/bone area) (/mm^2) and crack surface density (Cr.S.Dn = Cr.N × Cr.Le / bone area) (μm/mm^2).

2.4 Bone microarchitecture assessment by backscattered electron microscopy

The resin-embedded L4 vertebrae blocks prepared for microdamage analysis were cut with a saw, polished to a 1 µm diamond finish, then carbon coated. We used a scanning electron microscope (XL30; Philips/FEI, Oregon, USA) fitted with a backscattered electron detector (Philips/FEI). The signal was calibrated using C (Z = 6) and A1 (Z = 13), then the settings were changed to increase the contrast of the bone signal (Z = approx. 10). During the acquisition session, we controlled the drift of the signal using SiO_2 as a standard (only for slight adjustments). The accelerating voltage was 20 kV. Digital images were collected at 80× magnification; adjacent images were obtained on each block.

Image analysis was performed with a Quantimet 500 IW using Qwin Pro (Leica Microsystems, Cambridge, UK). The images were converted to binary images using a constant threshold of 85. The binary images were then skeletonized and pruned to quantify the number of nodes (/mm^2), number of termini (/mm^2), and different types of struts [32]. We calculated the lengths of node-to-node struts (mm/mm^2), node-to-terminus struts (mm/mm^2), and terminus-to-terminus struts (mm/mm^2), and the total strut length (mm/mm^2). Of these parameters, the increase in the number of nodes, node-to-node struts, and node-to-terminus struts can be related to the connectedness of the structure. Struts reaching the borders of the images were not considered except for the total strut length.

2.5 Collagen crosslink analysis

The procedure to analyze collagen crosslinks in bone after the density fractionation was as reported previously [27][29][30]. Briefly, density-fractionated bone powders of the third lumbar vertebrae were subjected to the collagen crosslink analysis. Fractionated bone powders were pooled into two fractions: low-density fraction (< 2.0 mg/mL) and high-density fraction (≥ 2.0 mg/mL). We defined the boundary line between the low- and high-density fractions at 2.0 mg/mL based on the report by Sodek et al.[31]. By separating bone at the 2.0 mg/mL boundary line, we obtained sufficient bone from both low- and high-density fractions for triplicate analyses of two different density fractions, suitable for estimating the collagen maturation process [29][30]. Toluene and bromoform used for the bone density fractionation do not affect the biochemical nature of bone collagen and its crosslinks [30].

Each sample of bone powder was demineralized twice with 0.5 M EDTA in 50 mM Tris buffer (pH 7.4) for 96 h at 4°C. The demineralized bone residues were then suspended in 0.15 M potassium phosphate buffer (pH 7.6) and reduced at 37°C with $NaBH_4$. The reduced specimens were hydrolyzed in 6 N HCl at 110°C for 24 h. Hydrolysates were analyzed for the content of crosslinks and hydroxyproline on a Shimadzu LC9 HPLC fitted with a cation exchange column (0.9 × 10 cm, Aa pack-Na; JASCO, Ltd., Tokyo, Japan) linked to an inline fluorescence flow monitor (RF10AXL; Shimadzu, Shizuoka, Japan). It was assumed that collagen weighed 7.5 times the measured hydroxyproline weight with a molecular weight of 300,000. The resulting data were used to calculate the cross-link values as mol/mol of collagen. Reducible immature divalent crosslinks (dehydrodihydroxylysinonorleucine, deH-DHLNL; dehydrohydroxylysinonorleucine, deH-HLNL; and dehydrolysinonorleucine, deH-LNL) were identified and quantified according to their respective reduced forms (dihydroxylysinonorleucine, DHLNL; hydroxylysinonorleucine, HLNL; and lysinonorleucine, LNL). The mature crosslinks and common amino acids such as hydroxyproline were detectable with post-column derivatization using *o*-phthalaldehyde, whereas the mature trivalent pyridinium crosslinks (pyridinoline, Pyr; and deoxypyridinoline, Dpyr) and the non-enzymatic crosslink pentosidine (Pen) were detected by natural fluorescence. The HPLC system we established enabled us to determine enzymatic and non-enzymatic crosslink contents within a linear range of 0.2 to 600 pmol in bone specimens. The total content of AGEs as well as pentosidine content was determined by the method of Tang et al.[35]. Briefly, AGE content was determined by using a fluorescence reader at 370 nm excitation and 440 nm emission (JASCO FP6200, JASCO) and normalized to a quinine sulfate standard. Data were expressed as mean ± standard deviation (SD).

2.6 Bone histology

Each animal had been subcutaneously injected with 8 mg/kg of calcein 15 days and 5 days prior to termination. L2 vertebrae were collected for bone histology. All bone samples were fixed in 10% neutral-buffered formalin for 3 days and transferred to 70% ethanol. Bones were then trimmed, dehydrated, and embedded in methyl methacrylate. Sagittal histological sections of L2 vertebrae were observed under a light microscope after toluidine blue staining for evaluating bone histology, or under a fluorescence microscope for visualizing calcein labeling (Nikon Eclipse E800; Nikon, Tokyo, Japan).

2.7 Statistical analysis

2.7.1 Density fractionation;

Data were analyzed as previously described [36]. The way to estimate if two distributions differ is to calculate the logit function of each distribution. For these experiments, the logit number of each sample is: ln(proportion of ≥ 2.00 mg/mL fraction) – ln(proportion of < 2.00 mg/mL fraction). The statistical analyses were performed using SPSS software (IBM, Armonk, NY, USA).

2.7.2 Bone microdamage assessment

Data from each experiment was evaluated separately using the SAS software package (SAS Institute, Inc., Cary, NC, USA). Group variance was evaluated using the Shapiro-Wilks test. If the assumption of normality was met ($p \geq 0.05$), a parametric two-tailed t-test was performed to determine differences between the control and treated groups. If the assumption of normality was not met, for either/both groups ($p < 0.05$), the non-parametric Wilcoxon-Mann-Whitney test (two-tailed) was used to compare the control and treated groups. Spearman's rank correlation coefficient method was used to analyze the correlation between the contents of Pen and total fluorescent AGEs in bone. For all comparisons, both parametric and non-parametric tests are reported, with $p < 0.05$ considered statistically significant.

2.7.3 Bone microarchitecture assessment

The statistical analyses were performed using SPSS software (IBM, Armonk, NY, USA). Independent Student's t-tests were done between the ELD treatment group and corresponding vehicle control group for each experiment. P-values less than 0.05 were considered significant.

2.7.4 Collagen crosslink analysis

Analysis of variance was performed using the SAS software package (SAS Institute). The significance of differences (in comparison with the OVX-vehicle control group) was determined using the Tukey-Kramer test. P-values less than 0.05 were considered statistically significant.

3. Results

3.1 Bone mineralization assessment by density fractionation

Treatment with 0.1 µg/kg or 0.3 µg/kg of ELD shifted the distribution profile of bone mineralization to a higher density compared with the corresponding vehicle controls (Fig. 1A, 1B). The average logit number of the ELD 0.3 µg/kg group and the OVX-Veh2 control group were -0.394 and 1.009, respectively (Fig. 1D). The shift in the value of the logit function between two groups was significant ($p = 0.0002$). The average logit number of the ELD 0.1 µg/kg group and the OVX-Veh1 were 1.439 and 1.842, respectively (Fig. 1C). But there was no significant difference between the value of the logit function of the ELD 0.1 µg/kg group and the OVX-Veh1 control group ($p = 0.270$).

3.2 Bone microdamage

There were no significant differences between the ELD 0.1 µg/kg group and OVX-Veh1 control group for any of the microdamage variables measured (Table 1). The ELD 0.3 µg/kg group had half as many cracks as the OVX-vehicle group ($p = 0.052$). When normalized for bone area, the ELD 0.3 µg/kg group had significantly lower crack density ($p = 0.027$) and crack surface density ($p = 0.049$) as compared to the OVX-Veh2 control group. There was no significant difference between groups for crack length (Table 1).

3.3 Bone microarchitecture

The results of the strut analysis of the trabecular bone from the L4 vertebrae are shown in Table 2. These data were derived from the backscattered electron microscopic images (Fig. 2). The results are consistent with increased trabecular connectivity as demonstrated by a higher number of nodes and node-to-node strut lengths as well as a lower number of termini and terminus-to-terminus strut lengths with both 0.1 µg/kg and 0.3 µg/kg of ELD.

3.4 Enzymatic and non-enzymatic collagen crosslinks

The total enzymatic crosslink content (the sum of DHLNL, HLNL, LNL, Pyr, and Dpyr) in both low- and high-density fractions from bones of the ELD-treated (0.1 and 0.3 µg/kg) groups were significantly higher than

those of the corresponding OVX-vehicle control groups (Fig. 3A, 3C, and Table 3). Notably, immature reduced forms of enzymatic crosslinks (DHLNL, HLNL, and LNL) significantly and markedly increased with ELD treatment, whereas increases in mature non-reducible forms of enzymatic crosslinks (Pyr and Dpyr) by the ELD treatment were significant but moderate (Table 3).

We calculated the biochemical collagen maturation index, defined as the ratio of total mature enzymatic crosslinks (Pyr+Dpyr) to total immature crosslinks (DHLNL+HLNL+LNL) [29][30][35] (Table 3). The maturation index showed a significant reduction in both low- and high-density fractions of bone from the ELD-treated groups compared with those from the corresponding OVX-vehicle control groups. Conversely, contents of Pen, the non-enzymatic AGE type of crosslink, were significantly lower in both low- and high-density fractions from bones of the ELD-treated groups than in those of the corresponding OVX-vehicle control groups (Fig. 3B, 3D, and Table 3).

Regarding total fluorescent AGEs, results similar to those of Pen are evident (Table 3). Pen is just a component of various AGEs, and because the content of Pen in bone correlates positively with the total amount of fluorescent AGEs, the measurement of Pen can be used as a surrogate marker of total AGE formation [37]. In this study, we also confirmed that there was a significant and positive correlation between the content of Pen and the total fluorescent AGEs in bone ($R^2 = 0.339$, $p < 0.0001$) (data not shown). The contents of the senescent crosslinking Pen and total contents of AGEs were significantly higher in the high-density fractions than in the low-density fractions in both the OVX-vehicle and ELD-treated groups (all $p < 0.05$, Table 3).

3.5 Bone histology

Trabecular bone sections of the ELD-treated cynomolgus monkeys demonstrated many “bud-like” bone formation patterns (Fig. 4A). Convex, bud-like focal deposits of bone matrix were observed on the smooth line forming the boundary to the underlying bone matrix. Bone specimens from the ELD-treated OVX monkeys revealed various bone buds labeled with continuous lines of calcein (Fig. 4B). No monkeys in the vehicle-treated control group in this study had such focal bone formation. These findings in the ELD-treated monkeys

283 are similar to the histological features of bone minimodeling found in our previous studies using ELD-
284 administered OVX rats [8][38].

285 **4. Discussion**

286 We have previously reported that ELD treatment for 6 months increased lumbar spine BMD, suppressed
287 ovariectomy-induced increases in bone turnover markers, and improved biomechanical parameters of lumbar
288 vertebrae in OVX cynomolgus monkeys [6]. Histomorphometrical analysis of bone revealed that both bone
289 formation and bone resorption parameters in the trabecular bones of the lumbar vertebrae were suppressed by
290 the ELD treatment. Therefore, we concluded that, in a bone-remodeling animal model, ELD increases BMD
291 and improves bone biomechanical properties, at least, in part, by normalizing bone turnover. In that study,
292 treatment with ELD at doses of 0.1 μg/kg and 0.3 μg/kg for 6 months increased lumbar spine (L1–L4) BMD
293 by 7.7% and 10.8%, respectively, compared to the corresponding OVX-vehicle controls, and increased the
294 peak load of intact L3 vertebra in a compression test by 26.4% and 84.2%, respectively. Those observations
295 indicated that the ELD treatment improved bone mechanical properties more than could be explained by the
296 increase in BMD. Comparing those results with the results from studies of other anti-osteoporotic agents in the
297 OVX monkey model, even though bisphosphonates such as clodronate, ibandronate, and minodronate
298 increased lumbar spine BMD by more than 10%–30%, they improved peak load in the compression test by
299 only approximately 30% [39][40][41].

300 Bone density fractionation of the vertebral body in the current study revealed that the ELD treatment
301 slightly shifted bone mineralization to a higher density. As previously reported, osteoid surface (OS/BS),
302 osteoid thickness (O.Th), and activation frequency (Ac.f) were reduced in the lumbar vertebral trabecular bone
303 of the ELD-treated groups compared with those of the OVX control groups [6]. However, ELD treatment did
304 not overly affect osteoid maturation time (Omt). These bone histomorphometrical data indicate that ELD does
305 not accelerate osteoid mineralization and facilitates secondary mineralization in the vertebral bone by slowing
306 down bone remodeling. Trabecular connectivity of the lumbar vertebra was increased by the ELD treatment.
307 Trabecular bones from ELD-treated groups had higher node-to-node strut length and lower terminus-to-

terminus strut length than did trabecular bones from the OVX control groups. In general, if BMD is equal, higher connectivity means a stronger bone. Therefore, improvement of trabecular connectivity in lumbar vertebrae may partly account for the improvement of biomechanical properties in compression.

There are several reports on the effects that various agents for the treatment of osteoporosis have on the material properties of bone. Long-term treatment with bisphosphonates has been shown to increase the accumulation of non-enzymatic AGE crosslinks and increase bone microdamage in canine trabecular bone [22] [42][43]. Damaged bone tissue is slowly resorbed by osteoclasts and replaced by new bone tissue during the bone remodeling process. When bone remodeling is suppressed with agents such as bisphosphonates, the microdamage in the old bone tissues accumulates due to both a reduction in the removal of damaged bone tissue and an increase in its formation. There is no concrete evidence that the levels of microdamage accumulation that occur *in vivo* weaken overall bone mechanical properties. We did not find increases in any parameters of bone microdamage in the bone specimens from the ELD-treated groups (Table 2) compared with those from OVX control groups. Rather, 0.3 μg/kg of ELD treatment reduced crack density and crack surface density of lumbar vertebral bones. Even though ELD treatment suppressed bone remodeling, it does not seem to increase the accumulation of bone microdamage. This favorable effect on microdamage may be due to there being no increase in the formation of AGEs in bone by the treatment with ELD.

Fibrillar type I collagen is the most abundant matrix protein in bone [3][22][29][30][34][44]. Stabilization of newly formed collagen fiber is initially achieved by the formation of covalent crosslinks between neighboring collagen molecules, and this covalent intermolecular crosslinking by post-translational modification is crucial for the stability of collagen fibrils. These collagen crosslinks can be divided into two types: crosslinks controlled by lysyl hydroxylase (LH) and lysyl oxidase (LOX) (enzymatic crosslinks) and AGE crosslinks (non-enzymatic crosslinks). Collagen crosslink formation is thought to affect the mechanical properties of bone at a material level. Impaired formation of enzymatic crosslinks and/or an increase in non-enzymatic crosslinks in bone collagen may contribute to the impaired bone mechanical properties seen in aging, osteoporosis, and diabetes mellitus [3][17][19][20][22][23][28][29][30]. Active vitamin D, calcitriol, has been shown to strongly upregulate gene expression of lysyl hydroxylases (LH1 and LH2b) and lysyl oxidase (LOXL2) in osteoblasts *in vitro* [45]. Treatment with the active vitamin D_3 analog alfacalcidol

335 stimulates LOX expression, and dose-dependently increases total enzymatic collagen crosslink content
336 (DHLNL, HLNL, LNL, Pyr, Dpyr) in tibial cortical bones of OVX rats *in vivo* [46]. We also demonstrated in a
337 fracture repair OVX rat model that alfacalcidol stimulated the formation of enzymatic crosslinks in callus
338 collagen, resulting in an increase of bone strength [22]. In the current study, ELD treatment increased the total
339 contents of enzymatic collagen crosslinks (DHLNL, HLNL, LNL, Pyr, Dpyr) in the lumbar vertebral bones of
340 cynomolgus monkeys, regardless of their bone mineralization status. This observation suggests that, similar to
341 calcitriol, ELD increases the production of both immature divalent and mature trivalent enzymatic crosslinks
342 by directly stimulating LH or LOX gene expression in bones. Therefore, ELD may be able to improve collagen
343 crosslinks in bones independently from bone turnover. We have reported that, in the OVX monkey model,
344 elevated enzymatic crosslink formation after treatment with teriparatide is an independent factor contributing
345 to increasing vertebral bone strength [16]. Therefore, the increase in the content of enzymatic crosslinks by
346 ELD treatment in the OVX primate model (Fig. 3 and Table 3) may contribute to increased bone strength [6].
347 The accumulation of young, newly formed collagen matrix by minimodeling may account for the observation
348 that accumulation of senescent types of crosslinking AGEs in bone after treatment with ELD is less than that in
349 bone from the OVX-vehicle control group.

350 Histological analysis of trabecular bone sections from ELD-treated cynomolgus monkeys showed bone
351 minimodeling, which is characterized by focal bone apposition directly to quiescent surfaces without prior
352 bone resorption, as reported previously in OVX rats [8]. At sites of minimodeling, the mineralization process
353 seems intact (Fig. 4). We do not know how this focal bone formation starts. However, small-size bone
354 formation may affect the bone microarchitecture, and may ultimately change the degree of mineralization of
355 trabecular bone.

356 One of the limitations in this study is the substantial differences exist in the biological parameters between
357 the two OVX-control groups due to the biological variability of nonhuman primates. For each experiment, we
358 selected animals from the colonies with the same criteria, and randomly assigned to either OVX-control group
359 or ELD-treated group. Thus, it is suitable to compare the results from the OVX-control group with those from
360 the ELD-treated group within the experiment. However, it may be difficult to discuss the dose-dependent
361 effects of ELD from this study. We believe this variability does not confound the interpretation of the data.

Other limitations are the absence of sham-operated control groups and the relatively short period of treatment. Not all of the measurements were performed on the same bone: Bone mechanical properties, bone mineralization, and collagen crosslinks were evaluated in L3 vertebrae; bone microdamage and bone microarchitecture were measured in L4 vertebrae; and assessment of bone histology was conducted with L2 vertebrae. Therefore, the improvement of bone mechanical properties seen in this study might not directly connect with the results from other analyses. Nevertheless, we can conclude that the increase in the degree of bone mineralization and the contents of enzymatic collagen crosslinks may partly contribute to the increased bone strength of the lumbar vertebral bone in OVX cynomolgus monkeys treated with ELD. We conclude that ELD provides positive effects on bone quality, complementing our earlier studies showing its positive effects on bone mass and strength.

5. Acknowledgments

This study was partly supported by a research grant from Chugai Pharmaceutical Co., Ltd. We thank all the members assigned to this project at Charles River Laboratories. The authors also wish to thank Dr. Keith Condon for the histological measurements used for microdamage analysis.

References

[1] Seeman E, Delmas PD. Bone quality—the material and structural basis of bone strength and fragility. N Engl J Med 2006;354:2250–61.

[2] Manolagas SC, Almeida M. Gone with the Wnts: beta-catenin, T-cell factor, forkhead box O, and oxidative stress in age-dependent diseases of bone, lipid, and glucose metabolism. Mol Endocrinol 2007;21:2605–14.

[3] Saito M, Marumo K. Collagen cross-links as a determinant of bone quality: a possible explanation for bone fragility in aging, osteoporosis, and diabetes mellitus. Osteoporos Int 2010;21:195–214.

[4] Uchiyama Y, Higuchi Y, Takeda S, Masaki T, Shira-Ishi A, Sato K, et al. ED-71, a vitamin D analog, is a more potent inhibitor of bone resorption than alfacalcidol in an estrogen-deficient rat model of osteoporosis. Bone 2002;30:582–8.

[5] Sakai S, Endo K, Takeda S, Mihara M, Shiraishi A. Combination therapy with eldecalcitol and alendronate has therapeutic advantages over monotherapy by improving bone strength. Bone 2012;50:1054–63.

[6] Smith SY, Doyle N, Boyer M, Chouinard L, Saito H. Eldecalcitol, a vitamin D analog, reduces bone turnover and increases trabecular and cortical bone mass, density, and strength in ovariectomized cynomolgus monkeys. Bone 2013;57:116–22.

[7] Harada S, Mizoguchi T, Kobayashi Y, Nakamichi Y, Takeda S, Sakai S, et al. Daily administration of eldecalcitol (ED-71), an active vitamin D analog, increases bone mineral density by suppressing RANKL expression in mouse trabecular bone. J Bone Miner Res 2012;27:461–73.

[8] de Freitas PH, Hasegawa T, Takeda S, Sasaki M, Tabata C, Oda K, et al. Eldecalcitol, a second-generation vitamin D analog, drives bone minimodeling and reduces osteoclastic number in trabecular bone of ovariectomized rats. Bone 2011;49:335–42.

[9] Kikuta J, Kawamura S, Okiji F, Shirazaki M, Sakai S, Saito H, et al. Sphingosine-1-phosphate-mediated osteoclast precursor monocyte migration is a critical point of control in antibone-resorptive action of active vitamin D. Proc Natl Acad Sci U S A. 2013;110:7009–13.

[10] Matsumoto T, Ito M, Hayashi Y, Hirota T, Tanigawara Y, Sone T, et al. A new active vitamin D3 analog, eldecalcitol, prevents the risk of osteoporotic fractures—a randomized, active comparator, double-blind study. Bone 2011;49:605–12.

[11] Ito M, Nakamura T, Fukunaga M, Shiraki M, Matsumoto T. Effect of eldecalcitol, an active vitamin D analog, on hip structure and biomechanical properties: 3D assessment by clinical CT. Bone 2011;49:328–34.

[12] Hagino H, Takano T, Fukunaga M, Shiraki M, Nakamura T, Matsumoto T. Eldecalcitol reduces the risk of severe vertebral fractures and improves the health-related quality of life in patients with osteoporosis. J Bone Miner Metab 2013;31:183–9.

[13] Matsumoto T, Takano T, Saito H, Takahashi F. Vitamin D analogs and bone: preclinical and clinical studies with eldecalcitol. Bonekey Rep 2014;3:513. doi: 10.1038/bonekey.2014.8.

[14] Jerome CP, Peterson PE. Nonhuman primate models in skeletal research. Bone 2001;29:1–6.

[15] Smith SY, Jolette J, Turner CH. Skeletal health: primate model of postmenopausal osteoporosis. Am J Primatol 2009;71:752–65.

[16] Saito M, Marumo K, Kida Y, Ushiku C, Kato S, Takao-Kawabata R, et al. Changes in the contents of enzymatic immature, mature, and non-enzymatic senescent cross-links of collagen after once-weekly treatment with human parathyroid hormone (1-34) for 18 months contribute to improvement of bone strength in ovariectomized monkeys. Osteoporos Int 2011;22:2373–83.

[17] Saito M, Fujii K, Mori Y, Marumo K. Role of collagen enzymatic and glycation induced cross-links as a determinant of bone quality in the spontaneously diabetic WBN/Kob rats. Osteoporos Int 2006;17:1514–23.

[18] Wang X, Shen X, Li X, Agrawal CM. Age-related changes in the collagen network and toughness of bone. Bone 2002;31:1–7.

[19] Oxlund H, Barckman M, Ortoft G, Andreassen TT. Reduced concentrations of collagen cross-links are associated with reduced strength of bone. Bone 1995;17:365S–71S.

[20] Banse X, Sims TJ, Bailey AJ. Mechanical properties of adult vertebral cancellous bone: correlation with collagen intermolecular cross-links. J Bone Miner Res 2002;17:1621–8.

[21] Saito M, Shiraishi A, Ito M, Sakai S, Hayakawa N, Mihara M, et al. Comparison of effects of alfacalcidol and alendronate on mechanical properties and bone collagen cross-links of callus in the fracture repair rat model. Bone 2010;46:1170–9.

[22] Saito M, Mori S, Mashiba T, Komatsubara S, Marumo K. Collagen maturity, glycation induced-pentosidine, and mineralization are increased following 3-year treatment with incadronate in dogs. Osteoporos Int 2008;19:1343–54.

[23] Vashishth D, Gibson GJ, Khoury JI, Schaffler MB, Kimura J, Fyhrie DP. Influence of nonenzymatic glycation on biomechanical properties of cortical bone. Bone 2001;28:195–201.

[24] Tang SY, Zeenath U, Vashishth D. Effects of non-enzymatic glycation on cancellous bone fragility. Bone 2007;40:1144–51.

[25] Saito M, Marumo K, Soshi S, Kida Y, Ushiku C, Shinohara A. Raloxifene ameliorates detrimental enzymatic and nonenzymatic collagen cross-links and bone strength in rabbits with hyperhomocysteinemia. Osteoporos Int 2010;21:655–66.

[26] Nojiri H, Saita Y, Morikawa D, Kobayashi K, Tsuda C, Miyazaki T, et al. Cytoplasmic superoxide causes bone fragility due to low-turnover osteoporosis with impaired collagen cross-linking. J Bone Miner Res 2011;26:2682–94.

[27] Saito M, Marumo K, Fujii K, Ishioka N. Single-column high-performance liquid chromatographic-fluorescence detection of immature, mature, and senescent cross-links of collagen. Anal Biochem 1997;253:26–32.

[28] Saito M, Kida Y, Kato S, Marumo K. Diabetes, collagen, and bone quality. Curr Osteoporos Rep 2014;12:181–8.

[29] Saito M, Fujii K, Marumo K. Degree of mineralization-related collagen crosslinking in the femoral neck cancellous bone in cases of hip fracture and controls. Calcif Tissue Int 2006;79:160–8.

[30] Saito M, Fujii K, Soshi S, Tanaka T. Reductions in degree of mineralization and enzymatic cross-links and increases in glycation-induced pentosidine in the femoral neck cortex in cases of femoral neck fracture. Osteoporos Int 2006;17:986–95.

[31] Sodek KL, Tupy JH, Sodek J, Grynpas MD. Relationship between bone protein and mineral in developing porcine long bone and calvaria. Bone 2000;26:189–98.

[32] Lundon K, Dumitriu M, Grynpas MD. Supraphysiologic levels of testosterone affect cancellous and cortical bone in the young female cynomolgus monkey. Calcif Tissue Int 1997;60:54–62.

[33] Grynpas MD, Hunter GK. Bone mineral and glycosaminoglycans in newborn and mature rabbits. J Bone Miner Res 1988;3:159–64.

[34] Allen MR, Iwata K, Phipps R, Burr DB. Alterations in canine vertebral bone turnover, microdamage accumulation, and biomechanical properties following 1-year treatment with clinical treatment doses of risedronate or alendronate. Bone 2006;39:872–9.

[35] Tang SY, Allen MR, Phipps R, Burr DB, Vashishth D. Changes in non-enzymatic glycation and its association with altered mechanical properties following 1-year treatment with risedronate or alendronate. Osteoporos Int 2009;20:887–94.

[36] Bracci PM, Bull SB, Grynpas MD. Analysis of compositional bone density data using log ratio transformations. Biometrics 1998;54:337–49.

[37] Karim L, Tang SY, Sroga GE, Vashishth D. Differences in non-enzymatic glycation and collagen cross-links between human cortical and cancellous bone. Osteoporos Int 2013;24:2441–7.

[38] Saito H, Takeda S, Amizuka N. Eldecalcitol and calcitriol stimulates 'bone minimodeling,' focal bone formation without prior bone resorption, in rat trabecular bone. J Steroid Biochem Mol Biol 2013;136:178–82.

[39] Itoh F, Kojima M, Furihata-Komatsu H, Aoyagi S, Kusama H, Komatsu H, et al. Reductions in bone mass, structure, and strength in axial and appendicular skeletons associated with increased turnover after ovariectomy in mature cynomolgus monkeys and preventive effects of clodronate. J Bone Miner Res 2002;17:534 –43.

[40] Smith SY, Recker RR, Hannan M, Müller R, Bauss F. Intermittent intravenous administration of the bisphosphonate ibandronate prevents bone loss and maintains bone strength and quality in ovariectomized cynomolgus monkeys. Bone 2003;32:45–55.

[41] Mori H, Tanaka M, Kayasuga R, Masuda T, Ochi Y, Yamada H, et al. Minodronic acid (ONO-5920/YM529) prevents decrease in bone mineral density and bone strength, and improves bone microarchitecture in ovariectomized cynomolgus monkeys. Bone 2008;43:840–8.

[42] Paschalis EP, Shane E, Lyritis G, Skarantavos G, Mendelsohn R, Boskey AL. Bone fragility and collagen cross-links. J Bone Miner Res 2004;19:2000–4.

[43] Mashiba T, Hirano T, Turner CH, Forwood MR, Johnston CC, Burr DB. Suppressed bone turnover by bisphosphonates increases microdamage accumulation and reduces some biomechanical properties in dog rib. J Bone Miner Res 2000;15:613–20.

[44] Yamauchi M. Collagen biochemistry: an overview. Singapore: World Scientific Publishing; 2002.

[45] Nagaoka H, Mochida Y, Atsawasuwan P, Kaku M, Kondoh T, Yamauchi M. 1,25(OH)2D3 regulates collagen quality in an osteoblastic cell culture system. Biochem Biophys Res Commun 2008;377:674–8.

[46] Nagaoka H, Terajima M, Yamada S, Azuma Y, Chida T, Yamauchi M. Alfacalcidol enhances collagen quality in ovariectomized rat bones. J Orthop Res. 2014;32:1030–6.

Figures and Tables

Table 1 Microdamage analysis of vertebral trabecular bone

	Crack number	Crack length (μm)	Crack density (/mm^2)	Crack surface density (μm/mm^2)
OVX-Veh1	10.6 ± 3.3	78.0 ± 3.6	1.21 ± 0.23	97.7 ± 21.0
ELD 0.1 μg/kg	14.2 ± 4.1	77.7 ± 2.2	1.63 ± 0.51	132.5 ± 43.6
	p = 0.496	p = 0.940	p = 0.464	p = 0.478
OVX-Veh2	20.8 ± 4.9	75.6 ± 3.2	2.06 ± 0.45	159.5 ± 36.2
ELD 0.3 μg/kg	10.1 ± 2.0	80.5 ± 3.8	0.92 ± 0.18	77.3 ± 17.1
	p = 0.052	p = 0.353	p = 0.027	p = 0.049

Data are represented as mean ± SEM. *P*-values less than 0.05 are considered statistically significant.

Table 2 Evaluation of trabecular connectivity in lumbar vertebrae

Experiment 1	OVX-Veh1	ELD 0.1 μg/kg	*P*-value
Number of termini (/mm^2)	2.55 ± 0.26	2.19 ± 0.19	0.253
Number of nodes (/mm^2)	1.68 ± 0.15	2.23 ± 0.15	0.020
Terminus to terminus strut length (mm/mm^2)	0.24 ± 0.02	0.13 ± 0.02	0.003
Node to terminus strut length (mm/mm^2)	0.78 ± 0.06	0.76 ± 0.04	0.771
Node to node strut length (mm/mm^2)	0.79 ± 0.10	1.12 ± 0.07	0.015
Total strut length (mm/mm^2)	2.00 ± 0.10	2.25 ± 0.09	0.088
Anisotropy ratio	0.80 ± 0.02	0.81 ± 0.01	0.622

Experiment 2	OVX-Veh2	ELD 0.3 μg /kg	*P*-value
Number of termini (/mm^2)	2.82 ± 0.12	1.89 ± 0.2	0.002
Number of nodes (/mm^2)	1.97 ± 0.09	2.3 ± 0.13	0.079
Terminus to terminus strut length (mm/mm^2)	0.24 ± 0.02	0.12 ± 0.02	0.002
Node to terminus strut length (mm/mm^2)	0.84 ± 0.02	0.78 ± 0.07	0.388
Node to node strut length (mm/mm^2)	0.82 ± 0.08	1.11 ± 0.08	0.025
Total strut length (mm/mm^2)	2.09 ± 0.07	2.2 ± 0.08	0.364
Anisotropy ratio	0.79 ± 0.02	0.81 ± 0.02	0.614

Data are presented as mean ± SEM. *P*-values less than 0.05 are considered statistically significant.

Table 3 Comparison of enzymatic and non-enzymatic crosslink contents between the OVX-vehicle controls and the ELD-treated groups

	Enzymatic crosslinks						Non-enzymatic crosslinks	
	Immature divalent forms (mol/mol of collagen)			Mature trivalent forms (mol/mol of collagen)		Collagen maturation index (Pyr+Dpyr) /(DHLNL+HLNL+LNL)	Total AGEs (ng quinine/mg of collagen)	Pentosidine (mmol/mol of collagen)
	DHLNL	HLNL	LNL	Pyr	Dpyr			
				Low-density fraction				
OVX-Veh1	0.522 ± 0.060	0.139 ± 0.031	2.131 ± 0.382	0.105 ± 0.007	0.018 ± 0.007	0.185 ± 0.015	129 ± 11.5	2.131 ± 0.382
ELD 0.1 μg/kg	0.636 ± 0.118*	0.260 ± 0.053*	1.753 ± 0.258*	0.132 ± 0.012*	0.035 ± 0.007*	0.189 ± 0.027	118.8 ± 11.8	1.753 ± 0.258*
				High-density fraction				
OVX-Veh1	0.466 ± 0.056	0.153 ± 0.028	2.742 ± 0.570$^{\#}$	0.103 ± 0.013	0.023 ± 0.009	0.202 ± 0.025	151.3 ± 30.0$^{\#}$	2.742 ± 0.570$^{\#}$
ELD 0.1 μg/kg	0.620 ± 0.182*	0.298 ± 0.078*	2.097 ± 0.349*	0.119 ± 0.007*,$^{\#}$	0.031 ± 0.005*	0.172 ± 0.045	141.1 ± 12.9$^{\#}$	2.097 ± 0.349*,$^{\#}$
				Low-density fraction				
OVX-Veh2	0.413 ± 0.075	0.150 ± 0.070	2.537 ± 0.588	0.112 ± 0.018	0.026 ± 0.011	0.249 ± 0.045	132.3 ± 14.0	2.537 ± 0.588
ELD 0.3 μg/kg	0.738 ± 0.133*	0.263 ± 0.063*	1.855 ± 0.448*	0.122 ± 0.016	0.044 ± 0.006*	0.169 ± 0.035*	110.0 ± 26.2*	1.855 ± 0.448*
				High-density fraction				
OVX-Veh2	0.410 ± 0.088	0.143 ± 0.063	2.943 ± 0.749	0.119 ± 0.018	0.029 ± 0.013	0.275 ± 0.046	161.0 ± 27.6$^{\#}$	2.943 ± 0.749
ELD 0.3 μg/kg	0.734 ± 0.161*	0.276 ± 0.077*	2.166 ± 0.417*	0.126 ± 0.016	0.037 ± 0.006$^{\#}$	0.165 ± 0.030*	140.5 ± 25.0$^{\#}$	2.166 ± 0.417*

Data are represented as mean ±SD.

*: $p < 0.05$ versus OVX-vehicle control.

$^{\#}$: $p < 0.05$ between low-density fraction and high-density fraction in the same treatment groups

Abbreviations: dihydroxylysinonorleucine, DHLNL; hydroxylysinonorleucine, HLNL; lysinonorleucine, LNL; pyridinoline, Pyr; deoxypyridinoline, Dpyr; pentosidine, Pen.

Figure 1. Distribution profiles of bone mineralization as assessed by density fractionation.

(A) Experiment 1: ELD 0.1 µg/kg group (grey bars) versus OVX-vehicle control (OVX-Veh1; white bars).

(B) Experiment 2: ELD 0.3 µg/kg group (grey bars) versus OVX-vehicle control (OVX-Veh2; white bars).

Data are presented as mean + SEM. Box-and-whisker plots show median, 25th and 75th quartiles, and complete data range of the logit numbers of Experiment 1**(C)** and Experiment 2 **(D)**

.

Figure 2. Backscattered electron microscopic imaging of the sagittal plane of lumbar vertebrae (L4).

(A) OVX-vehicle control (OVX-Veh1), **(B)** ELD 0.1 µg/kg group, **(C)** OVX-vehicle control (OVX-Veh2), **(D)** ELD 0.3 µg/kg group.

Figure 3. Collagen crosslinks in primate vertebral bone (L2). Bone samples were divided into low-density fraction (< 2.0 mg/mL) and high-density fraction (≥ 2.0 mg/mL).

(A) Total content of enzymatic crosslinks: the sum of immature (DHLNL, HLNL, LNL) and mature (Pyr, Dpyr) crosslinks in bone from the OVX-vehicle control (OVX-Veh1) and ELD 0.1 µg/kg group, **(B)** Content of non-enzymatic crosslink (Pen) in bone from the OVX-vehicle control (OVX-Veh1) and ELD 0.1 µg/kg group, **(C)** Total content of enzymatic crosslinks: the sum of immature (DHLNL, HLNL, LNL) and mature (Pyr, Dpyr) crosslinks in bone from the OVX-vehicle control (OVX-Veh2) and ELD 0.3 µg/kg group, **(D)** Content of non-enzymatic crosslink (Pen) in bone from the OVX vehicle control (OVX-Veh2) and ELD 0.3 µg/kg group.

Box-and-whisker plots show median, 25^{th} and 75^{th} quartiles, and complete data range.

Figure 4. Representative histological images of bone minimodeling. Trabecular bone sections of lumbar vertebrae from monkeys treated with ELD 0.3 μg/kg were observed under a light microscope or fluorescence microscope.

(A) Histological section with toluidine blue staining shows focal, convex bone (arrowheads)—indicative of minimodeling—forming on the smooth line of the underlying bone matrix (arrows). **(B)** Fluorescence microscopy image of an ELD-treated specimen. Note continuous, convex calcein labeling at the site of bone minimodeling (white arrow).

Scale bars, 100 μm.

Figure(s)

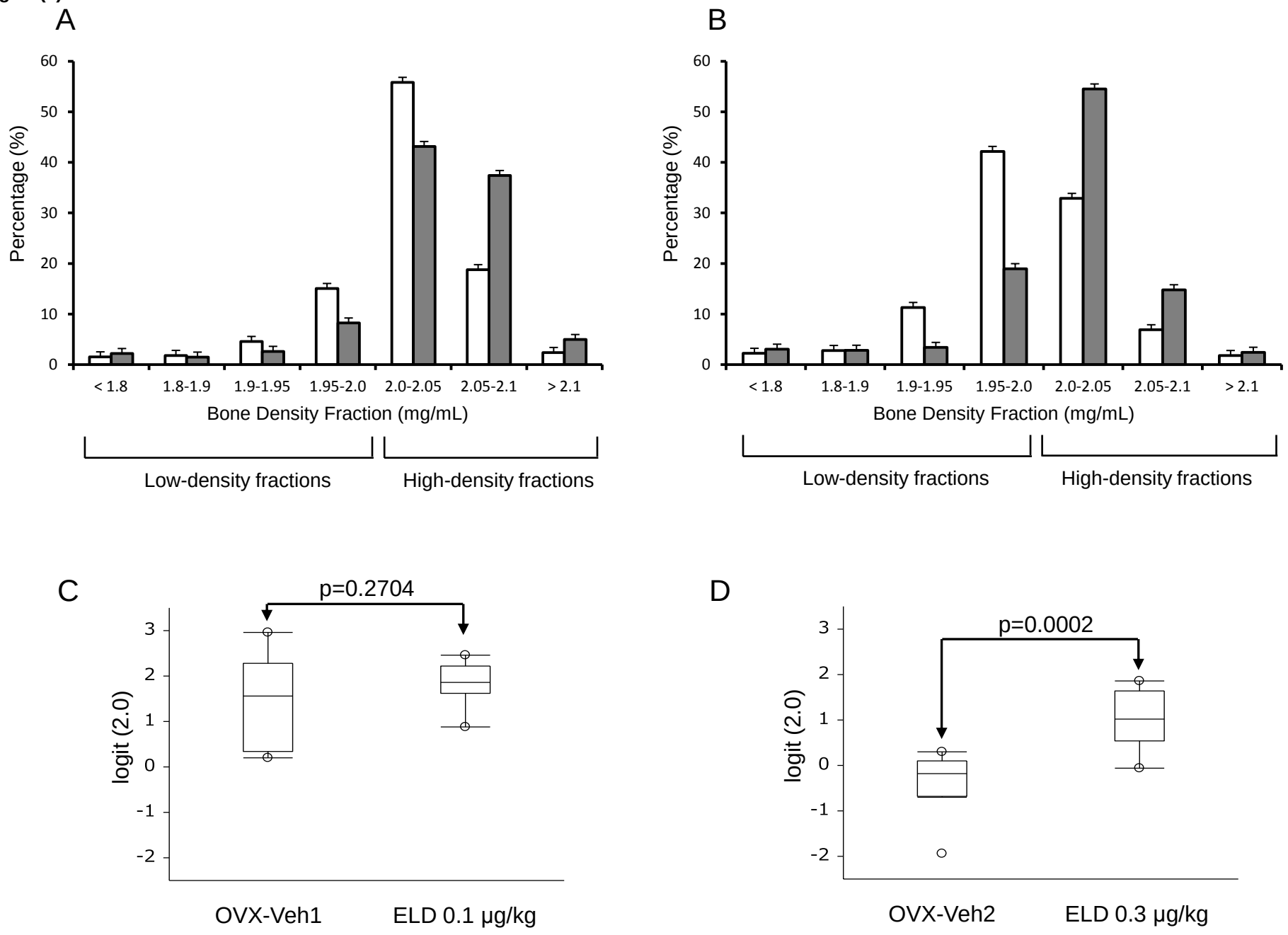

Fig.1

A: OVX-Veh1 B: ELD 0.1 μg/kg C: OVX-Veh2 D: ELD 0.3μg/kg

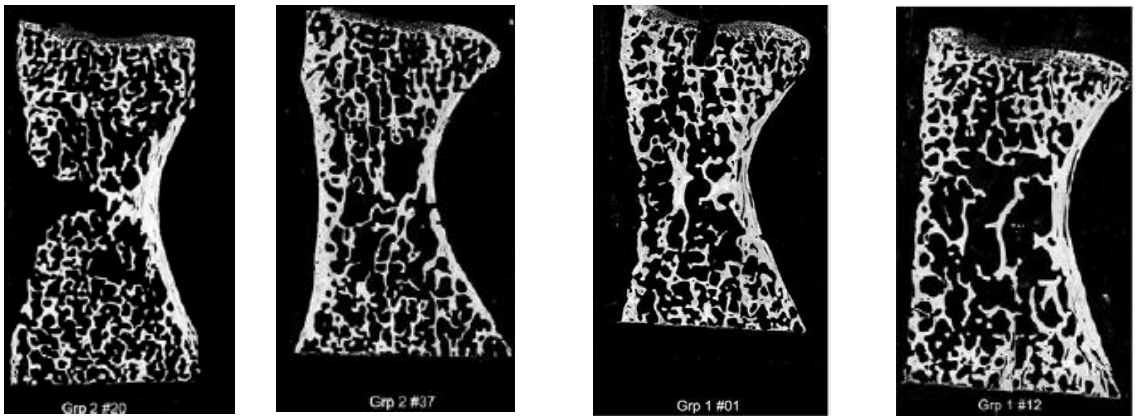

Fig. 2

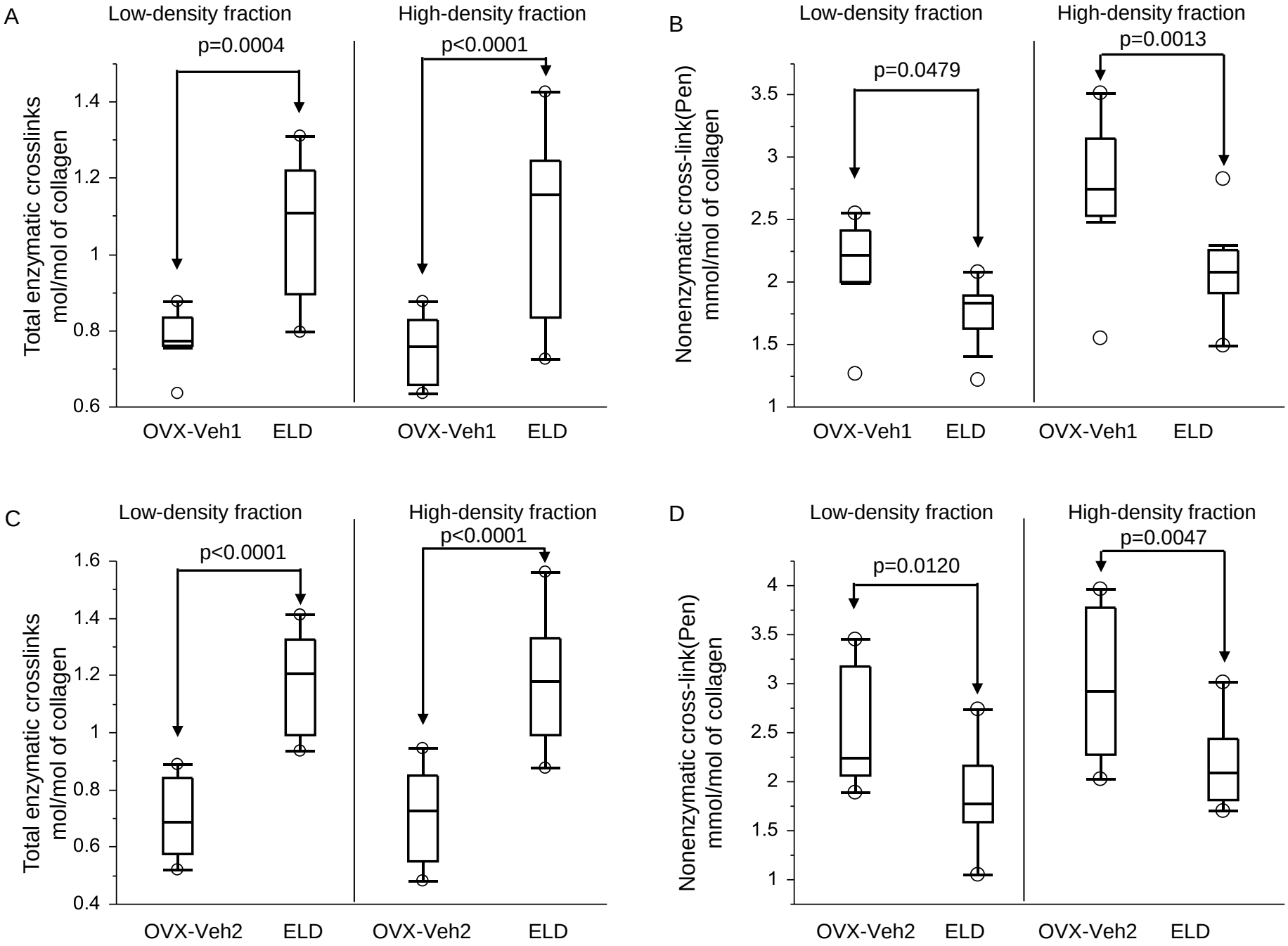
A
Low-density fraction
High-density fraction
p=0.0004
p<0.0001
Total enzymatic crosslinks
mol/mol of collagen
1.4
1.2
1
0.8
0.6
OVX-Veh1
ELD
OVX-Veh1
ELD
B
Low-density fraction
High-density fraction
p=0.0479
p=0.0013
Nonenzymatic cross-link(Pen)
mmol/mol of collagen
3.5
3
2.5
2
1.5
1
OVX-Veh1
ELD
OVX-Veh1
ELD
C
Low-density fraction
High-density fraction
p<0.0001
p<0.0001
Total enzymatic crosslinks
mol/mol of collagen
1.6
1.4
1.2
1
0.8
0.6
0.4
OVX-Veh2
ELD
OVX-Veh2
ELD
D
Low-density fraction
High-density fraction
p=0.0120
p=0.0047
Nonenzymatic cross-link(Pen)
mmol/mol of collagen
4
3.5
3
2.5
2
1.5
1
OVX-Veh2
ELD
OVX-Veh2
ELD

Fig. 3

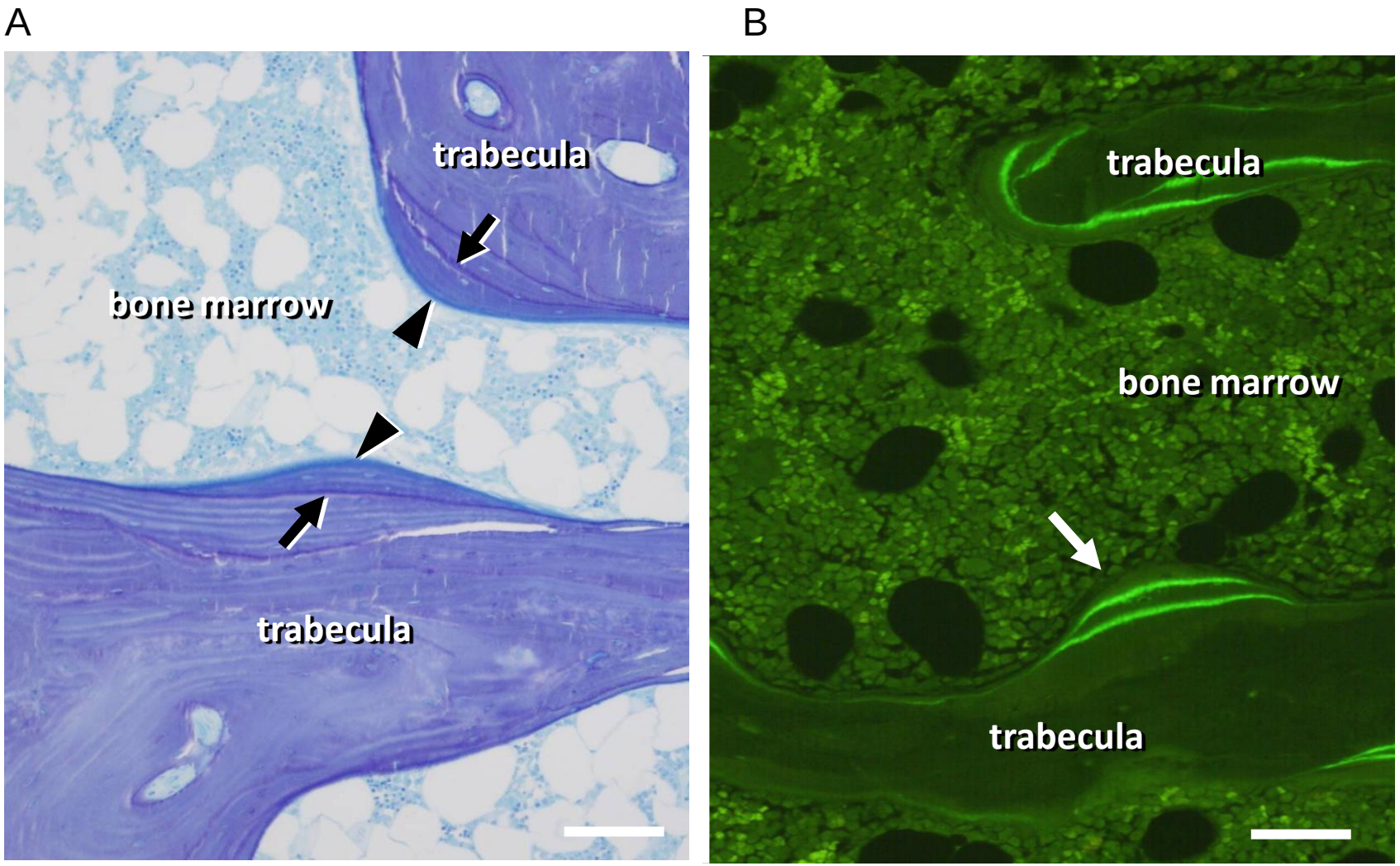
A
trabecula
bone marrow
trabecula
B
trabecula
bone marrow
trabecula

Fig.4